The Seventeenth International Symposium on Artificial Life and Robotics 2012 (AROB 17th '12),
B-Con Plaza, Beppu, Oita, Japan, January 19-21, 2012

Microscopic image restoration based on tensor factorization of rotated patches

Masayuki Kouno[1], Ken Nakae[1], Shigeyuki Oba[1,2], and Shin Ishii[1]

[1] Graduate School of Informatics, Kyoto University, Gokasho, Uji, Kyoto 611-0011, Japan
[2] PRESTO, Japan Science and Technology Agency
(Tel: 81-774-38-3938, Fax: 81-774-38-3941)
(kouno-m@sys.i.kyoto-u.ac.jp)

Abstract: In microscopic image processing for analyzing biological objects, structural characters of objects such as symmetry and direction can be used as a prior knowledge to improve the result. In this study, we incorporated filamentous character of local structures of neurons into a statistical model of image patches so as to obtain an image processing method based on tensor factorization with image patch rotation. Tensor factorization enabled us to incorporate correlation structure between neighboring pixels, and patch rotation helped us obtain image bases that well reproduce filamentous structures of neurons. We applied the proposed model to a microscopic image and found significant improvement in image restoration performance over existing methods even with smaller number of bases.

Keywords: Image processing, Microscopic image, Tensor factorization, Local feature extraction

1 INTRODUCTION

Statistical modeling of image patches is a standard method to extract local structural features in image processing [1]. Rectangular image patches are cut out from a target image and regarded as random vector-valued samples. Statistical modeling of vector-valued variables provides a general tool for statistical feature extraction, unsupervised learning, and noise reduction by regression, to various application fields, such as natural image recognition, text recognition, and face recognition [2]. On the other hand, such statistical methods may suffer from information loss due to conventional transformation from rectangular image patches into vectors, which would lead to deterioration of image restoration performance. In this study, we try to reduce loss of structural information in microscopic image processing, by introducing the following two strategies: to obtain direction of foreground objects by fitting rotational image patches; and, to handle each fitted image patch as a matrix *(patch height patch width)* rather than a vector.

2 NOTATIONS FOR TENSOR ANALYSIS

In this section, we introduce notations necessary to describe the idea of tensor factorization.

2.1 Tensor & its matricization

Let $\underline{\mathbf{Y}} \in \mathbb{R}^{I_1 \times I_2 \times \cdots \times I_N}$ be an an N-way tensor whose real-valued element $y_{i_1 i_2 \cdots i_N} \in \mathbb{R}$ is indexed by $i_n \in 1, 2, \quad , I_n$ for $1 \quad n \quad N$. Each of $I_1, I_2, \quad , I_N \in \mathbb{N}$ denotes the largest index number for the corresponding mode. A zero-way tensor is represented by a scalar y, a one-way tensor by a vector $\mathbf{y}$, a two-way tensor by a matrix $\mathbf{Y}$, and a three or higher-way tensor by a general tensor $\underline{\mathbf{Y}}$. $||\underline{\mathbf{Y}}||_{\mathrm{F}}^2$ denotes squared Frobenius norm, which is a sum of squared elements of the tensor $\underline{\mathbf{Y}}$.

To operate and illustrate a multi-way tensor, we may rearrange tensor elements to a matrix form, which is called matricization. The mode-n matricization of a tensor $\underline{\mathbf{Y}}$ rearranges the tensor elements as $\mathbf{Y}_{(n)} \in \mathbb{R}^{I_n \times (M_n)}$, where $M_n = I_1 I_2 \quad I_n \ {}_1 I_{n+1} \quad I_N$.

2.2 Tensor-matrix product

The mode-n product $(n = 1, 2, \quad , N)$ of a tensor $\underline{\mathbf{G}} \in \mathbb{R}^{J_1 \times J_2 \times \cdots \times J_N}$ and a matrix $\mathbf{A} \in \mathbb{R}^{I_n \times J_n}$, $\underline{\mathbf{Y}} = \underline{\mathbf{G}} \ {}_n \mathbf{A}$, is a tensor $\underline{\mathbf{Y}} \in \mathbb{R}^{J_1 \times \cdots \times J_{n-1} \times I_n \times J_{n+1} \times \cdots \times J_N}$ whose elements are given by $y_{j_1 j_2 \cdots j_{n-1} i_n j_{n+1} \cdots j_N} = \sum_{j_n=1}^{J_n} g_{j_1 j_2 \cdots J_N} a_{i_n j_n}$.

Multiplication of a tensor over all modes other than one mode is denoted as $\underline{\mathbf{G}} \ {}_{-n} \{\mathbf{A}\} = \underline{\mathbf{G}} \ {}_1\mathbf{A}^{(1)} \ {}_{n-1}\mathbf{A}^{(n-1)} \ {}_{n+1}\mathbf{A}^{(n+1)} \ {}_N\mathbf{A}^{(N)}$ and the resulting tensor has dimensionality $I_1 \quad I_n \ {}_1 \quad J_n \quad I_{n+1} \quad I_N$.

3 METHODS

In this section, we present our new image restoration method based on tensor factorization and rotational patches.

3.1 Image restoration incorporating patch rotation

Our image restoration method is a modification of the tensor factorization method proposed by Kim et al. [3]. Their method consisted of two steps; a basis learning step and a basis application step. We added a patch rotation process to both of these steps in order to incorporate symmetric structural features of image patch bases.

In the basis learning step, first, an image patch tensor is generated from an objective image; we obtain p samples of $m \quad m$ rectangular image patches from the full-size image; here, a rectangular image patch is said a foreground one if

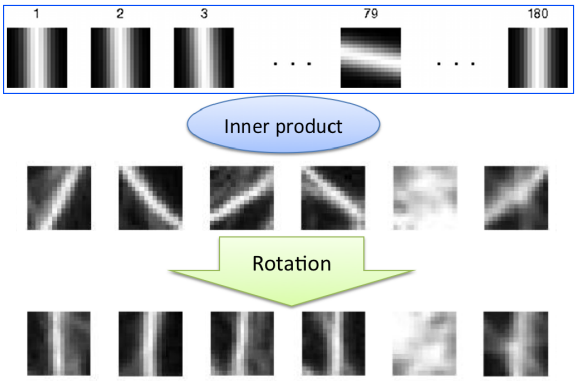

Fig. 1: Template image patch set by hand (leftmost panel) and its rotations (2...180). Foreground image patches before (middle) and after (lower) the rotation process.

its central pixel is brighter than the pre-determined level, or a background one otherwise. p samples of foreground patches are arranged into an $m \quad m \quad p$ three-way tensor, which is called a *train patch tensor*. Background patches were omitted in the following analysis. We calculate a *basis tensor* $\underline{\mathbf{U}} \in \mathbb{R}^{m \times m \times K}$ as a solution of the minimization problem:

$$\underline{\mathbf{U}} = \arg\min_{(\underline{\mathbf{U}}, \mathbf{V})} ||\underline{\mathbf{Y}} \quad \underline{\mathbf{U}} \quad {}_3\mathbf{V}||_{\mathrm{F}}^2, \tag{1}$$

where $\mathbf{V}$ is a $p \quad K$ mixing matrix such to allow the linear sum of K *basis patches* $\underline{\mathbf{U}}(:,:,k)(k = 1, \quad , K)$ to well approximate the *train patch tensor* $\underline{\mathbf{Y}}$; that is, the ith patch $\underline{\mathbf{Y}}(:,:,i)$ is well approximated by a linear sum of the basis patches $\sum_k \underline{\mathbf{U}}(:,:,k)\mathbf{V}(i,k)$ for all i. The number K $(< p)$ of basis patches should be set appropriately by hand. This minimization problem is solved by three-way tensor factorization and we applied higer order orthogonal iteration (HOOI) algorithm for it, which is explained in detail in section 3.2.

In the basis application process, we restore a noisy image patch $\boldsymbol{\mathcal{Y}}$ and achieve a restored image patch $\hat{\boldsymbol{\mathcal{Y}}}$ by applying the basis tensor $\underline{\mathbf{U}}$ that was obtained in the basis learning step. We assume that an image patch $\boldsymbol{\mathcal{Y}}$ is expressed by linear combination of K basis patches as follows.

$$\begin{aligned} \boldsymbol{\mathcal{Y}} &= \underline{\mathbf{U}} \quad {}_3\mathbf{v} + \mathbf{E} \\ &= \sum_{k=1}^{K} \underline{\mathbf{U}}(:,:,k) v_k + \mathbf{E}, \end{aligned} \tag{2}$$

where $\underline{\mathbf{U}}(:,:,k)$ is an $m \quad m$ matrix that represents the kth basis patch image, $\mathbf{v}$ is K-dimensional weight vector, and $\mathbf{E}$ is an $m \quad m$ residual matrix. We calculate the weight vector $\hat{\mathbf{v}}^T = (\hat{v}_1, \quad , \hat{v}_K)$ that minimizes the residual norm $||\mathbf{E}||_{\mathrm{F}}^2$. Finally, we obtain the restored image patch $\hat{\boldsymbol{\mathcal{Y}}} = \underline{\mathbf{U}} \quad {}_3\hat{\mathbf{v}}$. The entire image is restored by applying the above restoration process for all patches in the image.

Algorithm HOOI for three-way tensor factorization

Input: $\underline{\mathbf{Y}} \in \mathbb{R}^{I_1 \times I_2 \times I_3}$

Output: n th matrix $\mathbf{A}^{(n)} \in \mathbb{R}^{I_n \times J_n} (n = 1, 2, 3)$ and a core tensor $\underline{\mathbf{G}} \in \mathbb{R}^{J_1 \times J_2 \times J_3}$ such that $\left|\left|\underline{\mathbf{Y}} \quad \hat{\underline{\mathbf{Y}}}\right|\right|_{\mathrm{F}}^2$ is minimized.

1: **begin**
2: random initialization for all matrices $\mathbf{A}^{(n)}$
3: **repeat**
4: **for** $n = 1$ *to* 3 **do**
5: $\underline{\mathbf{W}}^{(n)} = \underline{\mathbf{Y}} \quad {}_n\{\mathbf{A}^{(n)T}\}$
6: $[\mathbf{A}^{(n)}, \mathbf{\Sigma}^{(n)}, \mathbf{B}^{(n)}] = \mathtt{svds}(\mathbf{W}_{(n)}^{(n)}, J_n)$
7: **end for**
8: **until** a stopping criterion is realized
9: $\underline{\mathbf{G}} = \underline{\mathbf{Y}} \quad {}_1\mathbf{A}^{(1)^T} \quad {}_2\mathbf{A}^{(2)^T} \quad {}_3\mathbf{A}^{(3)^T}$
10: **end**

In this study, we introduce a patch rotation process in order to incorporate symmetry in the objective cell structures. First, we prepared a template image (the leftmost panel in Fig. 1), which was set manually to represent a local neural filamentous structure in the vertical direction. Next, we prepared a set of its rotated image templates with rotation angles, $1, 2, ..., 180$ degree (Fig. 1). In the patch rotation process, we fit each sampled patch to the vertical template in the following manner; calculate correlation coefficients between the sampled patch and the rotated templates of 180 rotation angles, determine the best rotation angle that maximizes the correlation, and rotate the sampled patch into the inverse direction with the determined rotation angle. In the above procedure, we rotated the template patch 180 times, rather than the sampled patch, in order to reduce the number of total number of rotation operation. Fig. 1 shows some examples of image patches before (middle) and after (lower) the patch rotation.

We applied the patch rotation process to the both of basis learning and basis application steps. Before the basis learning step, we align all image patches to fit the template image, and gather the rotated patches to construct a three-way patch tensor for the basis learning. Before the basis application step, we align each image patch to fit the template image, and restore the central pixel of the result of an application of the base.

Owing to the patch rotation, we can omit trivial variations of foreground patch images that can be generated by the rotation of rectangular spatial cutting windows, and, consequently, we expect that the set of bases reflect variations among neuronal local structures.

3.2 HOOI algorithm for basis learning step

The HOOI algorithm for the three-way tensor factorization in the basis learning step is based on an iterative Al-

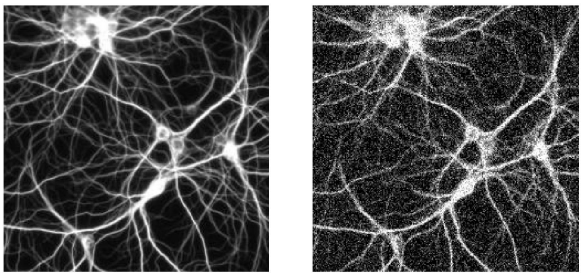

Fig. 2: An original microscopic image (size: 300 300 pixels) taken from `www.greenspine.ca` (Paul De Koninck, Laval University) (left) and a noisy image (right).

ternative Least Squares (ALS) algorithm. In each iteration of ALS, one basis is updated to minimize the residual error while keeping the others fixed, and finally we seek a (locally) optimal solution [4]. An extension of ALS for tensor factorization, HOOI was first introduced by De Lathauwer, De Moor and Vandewalle [4] and recently extended and implemented by Kolda and Bader in their MATLAB Tensor Toolbox[5]. We used this toolbox for tensor factorization in this study.

The HOOI factorizes the $m \quad m \quad p$ patch tensor $\underline{\mathbf{Y}}$ into an $m \quad m \quad K$ core tensor $\underline{\mathbf{G}}$ and three matrices $\mathbf{A}^{(1)}$, $\mathbf{A}^{(2)}$, and $\mathbf{A}^{(3)}$,

$$\underline{\mathbf{Y}} = \underline{\mathbf{G}} \quad {}_1\,\mathbf{A}^{(1)} \quad {}_2\,\mathbf{A}^{(2)} \quad {}_3\,\mathbf{A}^{(3)}. \tag{3}$$

We calculate the basis tensor that is defined in Eq. (1), $\underline{\mathbf{U}} \in \mathbb{R}^{m \times m \times K}$, by using the result of HOOI as follows, $\underline{\mathbf{U}} = \underline{\mathbf{G}} \quad {}_1\,\mathbf{A}^{(1)} \quad {}_2\,\mathbf{A}^{(2)}$.

In the HOOI algorithm, $\mathtt{svds}(\mathbf{W}^{(n)}_{(n)})$ denotes a singular value decomposition procedure that decomposes a matrix like $\mathbf{W}^{(n)}_{(n)} = \mathbf{A}^{(n)}\mathbf{\Sigma}^{(n)}\mathbf{B}^{(n)T}$. The cost function $\left|\left|\underline{\mathbf{Y}} \quad \hat{\underline{\mathbf{Y}}}\right|\right|^2_{\mathrm{F}}$ is monitored so that the algorithm is terminated when its difference from that in the last step is smaller than a constant (' a stopping criterion ' on line 8 in the algorithm).

3.3 Image restoration by matrix factorization

We compared the proposed method with simple matrix factorization and two-way tensor factorization. In the case of two-way tensor factorization, the train patch tensor is arranged to an $M \quad p$ matrix, where the column size $M = m^2$ corresponds to the number of pixels in an $m \quad m$ image patch. The M-dimensional patch vector $\mathbf{y}$ is represented by a linear combination of $K(\ll p)$ bases. $\mathbf{y} = \sum_{k=1}^{K} v_k \mathbf{u}_k + \boldsymbol{\varepsilon}$, where $\mathbf{u}_k$ is the kth M-dimensional basis vector, v_k is a scalar weight of the kth basis, and $\boldsymbol{\varepsilon}$ is an M-dimensional residual vector. Let $\mathbf{U} = (\mathbf{u}_1, \quad , \mathbf{u}_K)$ be an $M \quad K$ matrix that gathers all basis vectors $\mathbf{u}_k$. In the basis learning step, we obtain a basis matrix $\mathbf{U}$ that minimizes $||\boldsymbol{\varepsilon}||^2_{\mathrm{F}}$, and, in the basis application step, we calculate $\hat{\mathbf{v}}$ and $\hat{\mathbf{y}} = \mathbf{U}\hat{\mathbf{v}}$.

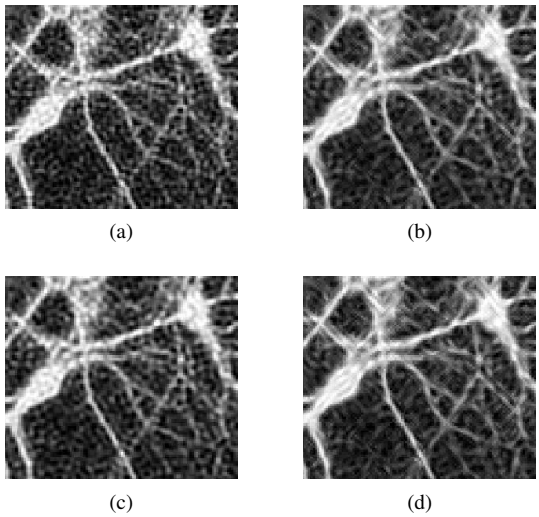

Fig. 3: Restoration by matrix factorization (a) without patch rotation ($K = 64$) and with patch rotation ($K = 52$). Restoration by tensor factorization (c) without patch rotation ($K = 52$) and(d) with patch rotation ($K = 46$).

4 RESULTS

Image restoration performance was compared between tensor factorization and matrix factorization, and between with and without the patch rotation process. A microscopic image of size 300 300 pixels was clipped from the original image (size: 634 800 pixels) of a neuronal network, registered on `www.greenspine.ca` (Paul De Koninck, Laval University) (Fig. 2, left). To examine the restoration performance, we artificially added white Gaussian noise (variance $= 0.03$) to the neuronal image (Fig. 2, right). Since we know the original image, we can evaluate the image restoration performance by calculating the root mean squared error (RMSE) of pixel brightness between the original and restored images. Since the performance depends on the number of bases, K, the RMSE was calculated with various K values for each method. For the basis learning, we extracted about 17,000 image patches of size 13 13 pixels from the original image before noise addition. Although the original image is not available in the actual image restoration application, we here assumed the basis learning has been accomplished by using clear images prior to the application of our image restoration method. Other possible procedure would be to iterate the basis learning step and image restoration by using the same (possibly noisy) images.

The image restoration results are shown in Fig. 3. The image restored by the tensor factorization with patch rotation obviously exhibited finer fiber structures than those by other methods. Such good restoration performance of the proposed method can be further seen in the numerical results summarized in Fig. 4. Since the performance was largely depen-

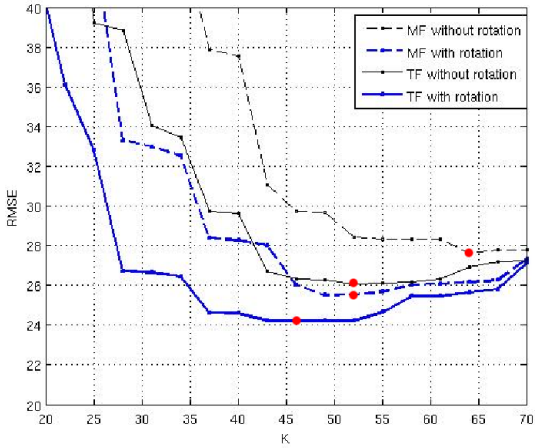

Fig. 4: Comparison of image restoration performance. Horizontal and vertical axes denote the number of bases (K) and the root mean squared restoration error (RMSE), respectively. Solid and chained lines denote the image restoration with and without image patch rotation process, respectively. Thick and thin lines denote the image restoration by means of three-way tensor factorization and matrix factorization, respectively. Red point denotes the best setting of K for each case.

dent on the number of bases, K, we here examined various K values. Although the RMSE of each method became the smallest with an appropriate setting of K, with the best setting being dependent on the method, the proposed method, the tensor factorization with patch rotation, showed the least RMSE value in every setting. In addition, tensor factorization (TF) showed better results that matrix factorization (MF), even though the former employed a smaller K value than the latter.

The advantage of the patch rotation was obvious especially when the number of bases was small. Table 1 shows the RMSE with the best setting of K for various noise levels added to the original image; our proposed method showed the best restoration performance with a smaller number of bases in all cases.

5 CONCLUDING REMARKS

In this study, we proposed an image restoration method based on the three-way tensor factorization of rotated image patches, which is suitable for restoration of microscopic images of biological targets such as neuronal networks. In the simulation experiment using a real image of neuronal network, we found significant performance gain in image restoration due to the two important ingredients of our method, tensor factorization and image patch rotation.

Fluorescence microscopy has a dilemma that increase in the frame rate suffers from larger shot noise, while decrease

Table 1: RMSE comparison for various noise levels added to the original image.

(a) variance $= 0.01$

RMSE	MF	TF
without rotation	18.27 ($K = 70$)	17.48 ($K = 64$)
with rotation	17.28 ($K = 64$)	**16.42** ($K = 55$)

(b) variance $= 0.03$

RMSE	MF	TF
without rotation	27.64 ($K = 64$)	26.09 ($K = 52$)
with rotation	25.51 ($K = 52$)	**24.21** ($K = 46$)

leads to the lack of information. Thus, a good image restoration technique is important for improving the data acquisition efficacy. For example, if we can restore low resolution images by utilizing basis images created from other high resolution images, the original low resolution images are restored cheaply in a software manner. Applications to 3D images and movies would be important future extensions, and capturing various finer structures of neuronal networks by further modifying our statistical model will also be promising.

ACKNOWLEDGMENT

This study was supported by Grant-in-Aid for Scientific Research on Innovative Areas: " Mesoscopic neurocircuity: towards understanding of the functional and structural basis of brain information processing " from MEXT, Japan.

REFERENCES

[1] Muresan DD and Parks TW (2003), Adaptive principal components and image denoising. *International Conference on Image Processing*, 1:I–101–4.

[2] Lee DD and Seung HS (1999), Learning the parts of objects by non-negative matrix factorization. *Nature*, 401(6755):788–91.

[3] Kim YD and Choi S (2007), Nonnegative Tucker Decomposition. *IEEE Conference on Computer Vision and Pattern Recognition*, 1–8.

[4] de Lathauwer L, de Moor B, and Vandewalle J (2000), On the Best Rank-1 and Rank-($R_1, R_2, ..., R_N$) Approximation of Higher-Order Tensors. *SIAM Journal on Matrix Analysis and Applications*, 21(4):1324–42.

[5] Bader BW and Kolda TG (2006), Algorithm 862: MATLAB tensor classes for fast algorithm prototyping. *ACM Trans. Mathematical Software*, 32(4):635—53.